Available online at www.sciencedirect.com
ScienceDirect
International Journal of Heat and Mass Transfer 49 (2006) 4893–4902
International Journal of HEAT and MASS TRANSFER
www.elsevier.com/locate/ijhmt

An iterative regularization method in estimating the base temperature for non-Fourier fins

Cheng-Hung Huang *, Hsin-Hsien Wu

Department of Systems and Naval Mechatronic Engineering, National Cheng Kung University, Tainan 701, Taiwan, ROC

Received 13 March 2006; received in revised form 24 May 2006
Available online 8 August 2006

Abstract

An inverse non-Fourier fin problem is examined in the present study by an iterative regularization method, i.e., conjugate gradient method (CGM), in estimating the unknown base temperature of non-Fourier fin based on the boundary temperature measurements. Results obtained in this inverse problem will be justified based on the numerical experiments where three different temperature distributions are to be determined. Results show that the inverse solutions can always be obtained with any arbitrary initial guesses of the base temperature. Moreover, the drawbacks of previous study for this identical inverse problem, such as (1) the inverse solutions become poor when the frequency of base temperature is increased, (2) the estimations depend strongly on the size of grids, (3) the estimations are sensitive to the measurement errors and (4) the uncertainty of using the concept of future time step, can all be avoided by applying this algorithm. Finally, it is concluded that accurate base temperatures can be estimated in the present study.

1. Introduction

Finned surfaces have been in use over a long period of time for dissipation of heat by convection or by radiation. Applications for finned surfaces are widely seen in air-conditioning, refrigeration, cryogenics and many cooling systems in industry. Therefore it is quite nature that many works have been done in order to study the thermal behaviors for these fins.

Numerous studies have been conducted to determine the thermal behaviors of the fins and to optimize the dimensions of the spine and longitudinal fins. A review on extended surfaces over six decades is available in the work by Kraus [1]. Yang [2] obtained the exact solution for convective fins under a periodic heat transfer. Eslinger and Chung [3] used a finite element method to solve a radiative and convective fin. Chung and Iyer [4] used an integral approach to determine the optimum dimensions for rectangular longitudinal fins and cylindrical pin fins. Yeh [5] used the Lagrange's multiplier method to find the optimum dimensions of longitudinal rectangular and cylindrical pin fins. In all the above fin problems only the Fourier effect are considered.

With advances in micro-fabrication technology, the micro-heat exchangers are of interest in many engineering applications, such as cooling of electronic chips and cryocoolers using helium II. For such a situation, phenomena with the finite thermal propagation speed might be important for the thermal analysis of the extended surface in the micro-heat exchangers.

For this reason, Lin [6] used a hybrid application of the Laplace transform and control volume methods in determining the non-Fourier fins performance under periodic thermal conditions. It can be seen that the discussions for thermal behaviors for the non-Fourier fins are still limited in the open literature and it is called the direct non-Fourier fin problems.

The direct non-Fourier fin problems are concerned with the determination of temperature at interior points of a fin when the fin shape, initial and boundary conditions and thermophysical properties are specified. In contrast, the

* Corresponding author. Tel.: +886 627 47018; fax: +886 627 47019.
E-mail address: chhuang@mail.ncku.edu.tw (C.-H. Huang).

0017-9310/$ - see front matter © 2006 Elsevier Ltd. All rights reserved.
doi:10.1016/j.ijheatmasstransfer.2006.05.033

Nomenclature

A	amplitude of the input temperature
b	thickness of the fin
C	specific heat capacity
f	unknown base temperature
J	functional defined by Eq. (4)
J'	gradient of functional defined by Eq. (13)
h_0	heat transfer coefficient
$h(x)$	spatial-dependent heat transfer coefficient
H	dimensionless heat transfer coefficient
k	thermal conductivity
L	length of the fin
M	number of the temporal measurements
P	direction of descent
t	temporal coordinate
T	temperature
T_b	periodic boundary condition
T_{in}	initial temperature of the fin
$\overline{T}_b$	mean temperature of the periodic boundary condition
T_e	environment temperature
x	spatial coordinate
Y	measured temperature

Greek symbols

β	dimensionless relaxation time
$\Delta\theta$	sensitivity function defined by Eq. (6)
ε	convergence criteria
γ	conjugate coefficient
η	dimensionless spatial coordinate
λ	adjoint function defined by Eq. (11)
μ	search step size
θ	dimensionless temperature
θ_e	dimensionless environment temperature
φ	random variable
ρ	density
σ	standard deviation of measurement error
τ	relaxation time
ω	dimensionless frequency of the temperature oscillation
$\hat{\omega}$	frequency of the temperature oscillation
ξ	dimensionless temporal coordinate

Superscript

n	iteration index

inverse non-Fourier fin problems considered here involves the determination of base temperature from the knowledge of temperature measurements taken at the fin tip.

The discussions on inverse hyperbolic problems can be found in the textbook by Isakov [7] and Romanov [8], but on the inverse non-Fourier fin problems are limited in the literature. Recently, Yang [9] published the first work regarding the estimation of fin base temperature with modified Newton–Raphson and future time steps methods for the non-Fourier fins. The immediately observed drawbacks of the estimated inverse solutions are (1) the inverse solutions become poor when the frequency of base temperature is increased, (2) the estimations depend strongly on the size of grids, (3) the estimations also depend strongly on the number of future time steps, where the optimum number for the future time steps is unknown in any real estimations, and (4) the inverse solutions are very sensitive to the measurement errors.

Inverse problems can be found in many engineering applications [10–21]. The technique of iterative regularization method [22] has been shown its potential for solving many kinds of inverse problems and has been applied to many different applications. For instance, Huang and Wang [23] used CGM in estimating surface heat fluxes for a three-dimensional inverse heat conduction problem. Huang and Chen [24] used same technique in estimating surface heat fluxes for a three-dimensional inverse heat convection problem. Huang and Huang [25] used CGM in an inverse biotechnology problem to estimate the optical diffusion and absorption coefficients of tissue. Huang and Lo [26] applied SDM in a three-dimensional inverse problem in predicting the heat fluxes distribution in the cutting tools. Huang and Shih [27] utilized the CGM in a shape identification problem to estimate simultaneously two interfacial configurations in a multiple region domain.

For this reason the objective of the present inverse study is to utilize the technique of the iterative regularization method, such as CGM, in the identical problem as was examined by Yang [9], and the goal is to avoid the drawbacks and to improve the accuracy of the inverse solutions.

The CGM is also called an iterative regularization method, which means the regularization procedure is performed during the iterative processes and thus the determination of optimal regularization conditions is not needed. The conjugate gradient method derives from the perturbation principles and transforms the inverse problem to the solution of three problems, namely, the direct, sensitivity and the adjoint problem, which will be discussed in detail in the following sections.

2. The direct problem

To illustrate the methodology for developing expressions for use in estimating the base temperature for non-Fourier fins based on the measured temperatures at the boundary, we consider the following fin problem.

The mathematical formulation of this transient non-Fourier fin problem in dimensional form is given by [6]:

$$\tau\rho C\frac{\partial^2 T}{\partial t^2}+\rho C\frac{\partial T}{\partial t}+2\tau\frac{h}{b}\frac{\partial}{\partial t}(T-T_e)=k\frac{\partial^2 T}{\partial x^2}-2\frac{h}{b}(T-T_e);\quad 0<x<L,\quad t>0 \tag{1a}$$

$$T(x,0)=T_{in};\quad 0<x<L,\quad t=0 \tag{1b}$$

$$\frac{\partial T(x,0)}{\partial t}=0;\quad 0<x<L,\quad t=0 \tag{1c}$$

$$T(0,t)=T_b=\overline{T}_b+A\cos(\hat{\omega}t)(\overline{T}_b-T_{in});\quad x=0,\quad t>0 \tag{1d}$$

$$\frac{\partial T(L,t)}{\partial x}=0;\quad x=L,\quad t>0 \tag{1e}$$

where k and ρC are the thermal conductivity and heat capacity per unit volume, respectively. τ is the relaxation time, T_{in} and T_b represent initial and base temperatures for the fin, $\overline{T}_b$ is the fin base mean temperature, A is the amplitude of the input temperature and $\hat{\omega}$ is the frequency of the temperature oscillation.

The heat transfer coefficient $h(x)$ is dependent on the spatial coordinate and is defined as

$$h(x)=h_0 H\left(\frac{x}{L}\right) \tag{2}$$

Here, h_0 is the referenced heat transfer coefficient and is defined as $h_0=bk/2L^2$. Fig. 1 illustrates the dimensional geometry for the non-Fourier fin considered here. If the following dimensionless quantities are defined

$$\theta=\frac{T-T_{in}}{T_b-T_{in}};\quad \theta_e=\frac{T_e-T_{in}}{T_b-T_{in}};\quad \eta=\frac{x}{L};\quad \xi=\frac{\alpha t}{L^2};$$
$$\beta=\frac{\alpha\tau}{L^2};\quad \omega=\frac{\hat{\omega}L}{\alpha}$$

The dimensionless non-Fourier fin equation can be expressed as

$$\beta\frac{\partial^2\theta}{\partial\xi^2}+(1+\beta H)\frac{\partial\theta}{\partial\xi}=\frac{\partial^2\theta}{\partial\eta^2}-H\theta+H\theta_e;\quad 0<\eta<1,\quad \xi>0 \tag{3a}$$

$$\theta(\eta,0)=0;\quad 0<\eta<1,\quad \xi=0 \tag{3b}$$

$$\frac{\partial\theta(\eta,0)}{\partial\xi}=0;\quad 0<\eta<1,\quad \xi=0 \tag{3c}$$

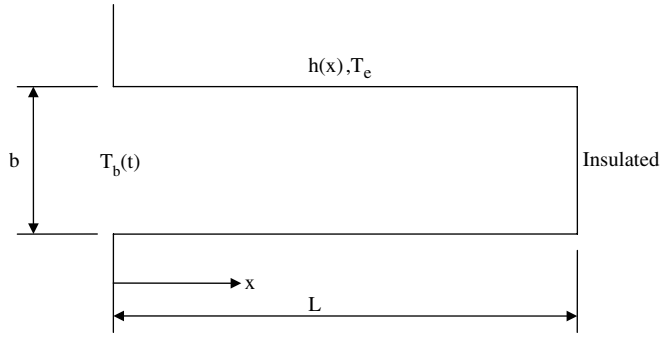

Fig. 1. The fin configuration.

$$\theta(0,\xi)=1+A\cos(\omega\xi)=f(\xi)=\text{unknown};\quad \eta=0,\quad \xi>0 \tag{3d}$$

$$\frac{\partial\theta(1,\xi)}{\partial\eta}=0;\quad \eta=1,\quad \xi>0 \tag{3e}$$

The direct problem considered here is concerned with the determination of temperature distribution of fins when the shape of fin, initial condition and the boundary conditions at both boundaries are known. The solution for the above non-Fourier fin problem is solved using Crank–Nicolson type central difference [28].

3. The inverse design problem

For the inverse problem, time-dependent base temperature, i.e., $f(\xi)$, is regarded as being unknown, but everything else in Eq. (3) is known. In addition, the temperatures measured at fin tip are assumed available.

Let the temperature reading taken by sensors at $\eta=1$ be denoted by $Y(1,\xi)$, it is noted that the measured temperature $Y(1,\xi)$ contain measurement errors. Then the inverse problem can be stated as follows: by utilizing the above mentioned measured temperature data $Y(1,\xi)$, estimate the unknown base temperature $f(\xi)$.

The solution of the present inverse problem is to be obtained in such a way that the following functional is minimized:

$$J[f(\xi)]=\int_{\xi=0}^{\xi_f}[\theta(1,\xi)-Y(1,\xi)]^2\,d\xi \tag{4}$$

here, $\theta(1,\xi)$ is the estimated or computed temperatures at $\eta=1$ and time ξ, ξ_f is the final time. These quantities are determined from the solution of the direct problem given previously by using an estimated temperature for the exact $f(\xi)$.

The conjugate gradient method has the ability in optimizing the above inverse problem and will be discussed in detail in next section.

4. Conjugate gradient method (CGM) for minimization

The following iterative process based on the CGM [22] is now used for the estimation of the unknown base temperature $f(\xi)$ by minimizing the functional $J[f(\xi)]$.

$$f^{n+1}(\xi)=f^n(\xi)-\mu^n P^n(\xi) \tag{5a}$$

Here, μ^n is the search step size in going from iteration n to iteration $n+1$ and $P^n(\xi)$ is the direction of descent (i.e., search direction) given by

$$P^n(\xi)=J'^n(\xi)+\gamma^n P^{n-1}(\xi) \tag{5b}$$

which is a conjugation of the gradient in the outward normal direction $J'^n(\xi)$ at iteration n and the direction of descent $P^{n-1}(\xi)$ at iteration $n-1$. The conjugate coefficient is defined as [20]

$$\gamma^n=\frac{\int_{\xi=0}^{\xi_f}(J'^n)^2\,d\xi}{\int_{\xi=0}^{\xi_f}(J'^{n-1})^2\,d\xi};\quad \text{with } \gamma^0=0 \tag{5c}$$

We note that when $\gamma^n = 0$ for any n, in Eq. (5b), the direction of descent $P^n(\xi)$ becomes the gradient direction, i.e., the steepest descent method (SDM) is obtained. The convergence of the above iterative procedure in minimizing the functional J is guaranteed in [29].

To perform the iterations according to Eq. (5a), we need to compute a step size μ^n and the gradient of the functional $J^n(\xi)$. In order to develop expressions for the determination of these two quantities, a "sensitivity problem" and an "adjoint problem" are constructed as described below.

5. Sensitivity problem and search step size

The sensitivity problem is obtained from the original direct problem defined by Eq. (3) in the following manner: It is assumed that when $f(\xi)$ undergoes a variation $\Delta f(\xi)$, $\theta(\eta, \xi)$ is perturbed by $\Delta\theta(\eta, \xi)$. Then replacing in the direct problem $f(\xi)$ by $f(\xi) + \Delta f(\xi)$ and $\theta(\eta, \xi)$ by $\theta(\eta, \xi) + \Delta\theta(\eta, \xi)$, subtracting the resulting expressions from the direct problem and neglecting the second-order terms, the following sensitivity problem for the sensitivity function $\Delta\theta(\eta, \xi)$ are obtained.

$$\beta\frac{\partial^2\Delta\theta}{\partial\xi^2} + (1+\beta H)\frac{\partial\Delta\theta}{\partial\xi} = \frac{\partial^2\Delta\theta}{\partial\eta^2} - H\Delta\theta; \quad 0<\eta<1, \quad \xi>0 \tag{6a}$$

$$\Delta\theta(\eta,0) = 0; \quad 0<\eta<1, \quad \xi = 0 \tag{6b}$$

$$\frac{\partial\Delta\theta(\eta,0)}{\partial\xi} = 0; \quad 0<\eta<1, \quad \xi = 0 \tag{6c}$$

$$\Delta\theta(0,\xi) = \Delta f(\xi); \quad \eta = 0, \quad \xi>0 \tag{6d}$$

$$\frac{\partial\Delta\theta(1,\xi)}{\partial\eta} = 0; \quad \eta = 1, \quad \xi>0 \tag{6e}$$

The technique of Crank–Nicolson type central difference discretization [28] is used to solve this sensitivity problem.

The functional $J(f^{n+1})$ for iteration $n+1$ is obtained by rewriting Eq. (5a) as

$$J(f^{n+1}) = \int_{\xi=0}^{\xi_f}[\theta(1,\xi;f^n - \mu^n P^n) - Y(1,\xi)]^2\,d\xi \tag{7a}$$

where we replaced f^{n+1} by the expression given by Eq. (5a). If temperature $\theta(1, \xi; f^n - \mu^n P^n)$ is linearized by a Taylor expansion, Eq. (7a) takes the form

$$J(f^{n+1}) = \int_{\xi=0}^{\xi_f}[\theta(1,\xi;q^n) - \mu^n\Delta\theta(1,\xi;P^n) - Y(1,\xi)]^2\,d\xi \tag{7b}$$

where $\theta(1,\xi;q^n)$ is the solution of the direct problem by using estimate base temperature for exact $f(0, \xi)$ at $\eta = 0$ and time ξ. The sensitivity functions $\Delta\theta(1, \xi;P^n)$ are taken as the solutions of problem (6) at the measured position $\eta = 1$ and time ξ by letting $\Delta f = P^n$. The search step size μ^n is determined by minimizing the functional given by Eq. (7b) with respect to μ^n. The following expression results:

$$\mu^n = \frac{\int_{\xi=0}^{\xi_f}[\theta(1,\xi) - Y(1,\xi)]\Delta\theta(1,\xi)\,d\xi}{\int_{\xi=0}^{\xi_f}[\Delta\theta(1,\xi)^2]\,d\xi} \tag{8}$$

6. Adjoint problem and gradient equation

To obtain the adjoint problem, Eq. (3a) is multiplied by the Lagrange multiplier (or adjoint function) $\lambda(\eta, \xi)$ and the resulting expression is integrated over the correspondent space and time domains. Then the result is added to the right hand side of Eq. (4) to yield the following expression for the functional $J[f(\xi)]$:

$$J[f(\xi)] = \int_{\xi=0}^{\xi_f}[\theta(1,\xi) - Y(1,\xi)]^2\,d\xi + \int_{\xi=0}^{\xi_f}\int_{\eta=0}^{1}\lambda(\eta,\xi)\left[\beta\frac{\partial^2\theta}{\partial\xi^2} + (1+\beta H)\frac{\partial\theta}{\partial\xi} - \frac{\partial^2\theta}{\partial\eta^2} + H\theta - H\theta_e\right]d\eta\,d\xi \tag{9}$$

The variation ΔJ is obtained by perturbing f by $f + \Delta f$ and θ by $\theta + \Delta\theta$ in Eq. (9), subtracting the resulting expression from the original Eq. (9) and neglecting the second-order terms. We thus find

$$\Delta J[f(\xi)] = \int_{\xi=0}^{\xi_f}2[\theta(1,\xi) - Y(1,\xi)]\Delta\theta\,d\xi + \int_{\xi=0}^{\xi_f}\int_{\eta=0}^{1}\lambda(\eta,\xi)\left[\beta\frac{\partial^2\Delta\theta}{\partial\xi^2} + (1+\beta H)\frac{\partial\Delta\theta}{\partial\xi} - \frac{\partial^2\Delta\theta}{\partial\eta^2} + H\Delta\theta\right]d\eta\,d\xi \tag{10}$$

In Eq. (10), the double integral terms are integrated by parts; the boundary conditions of the sensitivity problem are utilized. The vanishing of the integrands leads to the following adjoint problem for the determination of $\lambda(\eta, \xi)$:

$$\beta\frac{\partial^2\lambda}{\partial\xi^2} - (1+\beta H)\frac{\partial\lambda}{\partial\xi} - \frac{\partial^2\lambda}{\partial\eta^2} + H\lambda = 0; \quad 0<\eta<1, \quad \xi>0 \tag{11a}$$

$$\lambda(\eta,\xi_f) = 0; \quad 0<\eta<1, \quad \xi = \xi_f \tag{11b}$$

$$\frac{\partial\lambda(\eta,\xi_f)}{\partial\xi} = 0; \quad 0<\eta<1, \quad \xi = \xi_f \tag{11c}$$

$$\lambda(0,\xi) = 0; \quad \eta = 0, \quad \xi>0 \tag{11d}$$

$$\frac{\partial\lambda(1,\xi)}{\partial\eta} = -2[\theta(1,\xi) - Y(1,\xi)]; \quad \eta = 1, \quad \xi>0 \tag{11e}$$

The adjoint problem is different from the standard initial value problems in that the final time conditions at time $\xi = \xi_f$ is specified instead of the customary initial condition. However, this problem can be transformed to an initial value problem by the transformation of the time variables as $\chi = \xi_f - \xi$. Crank–Nicolson type central difference discretization [28] can then be used to solve the above adjoint problem.

Finally, the following integral term is left

$$\Delta J = \int_{\xi=0}^{\xi_f} \frac{\partial \lambda(0,\xi)}{\partial \eta} \Delta f \, d\xi \tag{12a}$$

From definition [22], the functional increment can be presented as

$$\Delta J = \int_{\xi=0}^{\xi_f} J'[f(\xi)] \Delta f(0,\xi) \, d\xi \tag{12b}$$

A comparison of Eqs. (12a) and (12b) leads to the following expression for the gradient of functional $J'[f(\xi)]$ of the functional $J[f(\xi)]$:

$$J'[f(\xi)] = \frac{\partial \lambda(0,\xi)}{\partial \eta} \tag{13}$$

The calculation of gradient equations is the most important part of CGM since it plays a significant role of the inverse calculation. We note that $J'[f(\xi)]$ is always equal to zero since $\lambda(\eta, \xi_f) = 0$ at $\xi = \xi_f$. With this fact and Eqs. ((5a)–(5c)) we concluded that the estimated value for $f(\xi)$ is definitely equal to the values of its initial guess.

One easy way to improve the prediction at end time ξ_f is to extend the measurement time. For instance, if end time $\xi_f = 10$, we should measure the data up to, say, $\xi = 12$ and then perform the inverse calculations. Finally extract the inverse solutions to $\xi_f = 10$. The singularity near ξ_f can greatly be improved.

7. Stopping criterion

If the problem contains no measurement errors, the traditional check condition is specified as

$$J[f^{n+1}(\xi)] < \varepsilon \tag{14a}$$

where ε is a small-specified number. However, the measured temperature data must contain measurement errors. Therefore, we do not expect the functional Eq. (4) to be equal to zero at the final iteration step. Following the experiences of the authors [22–27], the discrepancy principle is used as the stopping criterion, i.e., it is assumed that the temperature residuals may be approximated by

$$\theta(1,\xi) - Y(1,\xi) \approx \sigma \tag{14b}$$

where σ is the standard deviation of the measurements, which is assumed to be a constant. Substituting Eq. (14b) into Eq. (4), the following expression is obtained for stopping criteria ε:

$$\varepsilon = \sigma^2 \xi_f \tag{14c}$$

Then, the stopping criterion is given by Eq. (14a) with ε determined from Eq. (14c).

8. Computational procedure

The computational procedure for the solution of this inverse non-Fourier fin problem using conjugate gradient method may be summarized as follows:

Suppose $f^n(\xi)$ is available at iteration n.

Step 1. Solve the direct problem given by Eq. (3) for $\theta(\eta, \xi)$.
Step 2. Examine the stopping criterion given by Eq. (14a) with ε given by Eq. (14c). Continue if not satisfied.
Step 3. Solve the adjoint problem given by Eq. (11) for $\lambda(\eta, \xi)$.
Step 4. Compute the gradient of the functional $J'[f(\xi)]$ from Eq. (13).
Step 5. Compute the conjugate coefficient γ^n and direction of descent P^n from Eqs. (5c) and (5b), respectively.
Step 6. Set $\Delta f = P^n$, and solve the sensitivity problem given by Eq. (6) for $\Delta\theta(\eta, \xi)$.
Step 7. Compute the search step size μ^n from Eq. (8).
Step 8. Compute the new estimation for f^{n+1} from Eq. (5a) and return to step 1.

9. Results and discussion

The objective of this article is to show the validity of the CGM in estimating the base temperature $f(\xi)$ for non-Fourier fins accurately with no prior information on the functional form of the unknown quantities.

Before studying the inverse non-Fourier fin problem one should make sure first that the numerical solution for the direct problem is correct and accurate, otherwise the discussions of the inverse solutions will become meaningless. To test the accuracy of the direct problem, a benching mark problem [6] is first considered, i.e., solve Eq. (3) by using the following conditions [6]:

$$H(\eta) = e^{\eta}, \quad A = 0.5 \text{ and } \theta_e = 1.0$$

The numerical solutions for θ utilizing the technique of Crank–Nicolson type central difference [28] at $\xi = 0.5$ and $\omega = 1$ using $\beta = 0$, 1, 2 and 5 are shown in Fig. 2a. The temperature distributions at $\xi = 0.5$ and $\beta = 1$ using

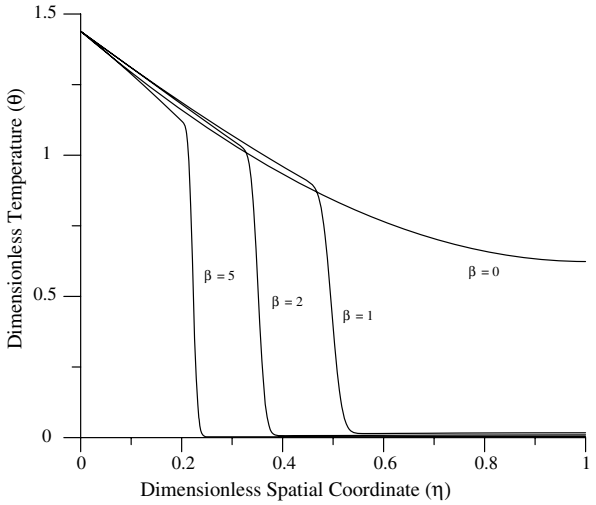

Fig. 2a. Temperature distributions for various values of β ($\omega = 1$ and $\xi = 0.5$).

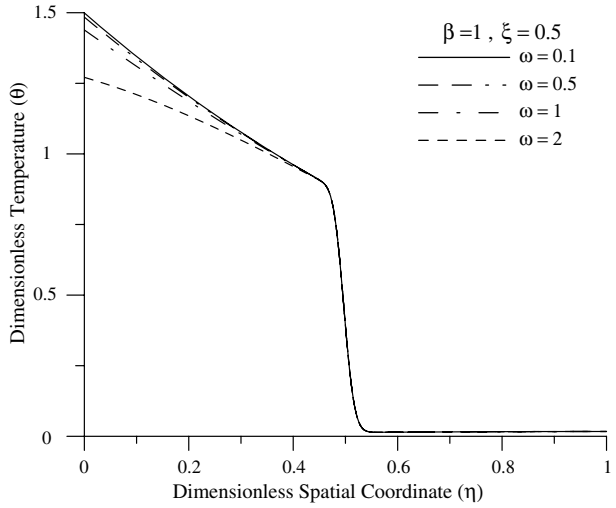

Fig. 2b. Temperature distributions for various values of ω ($\beta = 1$ and $\xi = 0.5$).

$\omega = 0.1$, 0.5, 1 and 2 are shown in Fig. 2b. The numerical solution is indeed accurate when comparing with the exact solution shown in reference [6]. Moreover, the oscillatory behavior for the numerical solution reported in reference [9] is greatly improved. This implies that more reliable inverse solution can be obtained by using the present numerical scheme. Finally the verification of our numerical program for direct problem is thus completed.

To illustrate the accuracy of the conjugate gradient method in predicting base temperature $f(\xi)$ for non-Fourier fins with the present inverse analysis from the knowledge of transient temperature recordings, three specific examples having different form of base temperatures are considered here.

In order to compare the results for situations involving random measurement errors, a normally distributed uncorrelated error with zero mean and constant standard deviation are considered. The simulated inexact measurement data $\mathbf{Y}$ can be expressed as

$$\mathbf{Y} = \mathbf{Y}_{\text{exact}} + \varphi\sigma \tag{15}$$

where $\mathbf{Y}_{\text{exact}}$ is the solution of the direct problem with an exact base temperature $f(\xi)$; σ is the standard deviation of the measurements; and φ is a random variable that generated by subroutine DRNNOR of the IMSL [30] and will be within -2.576 to 2.576 for a 99% confidence bound.

In all the test cases considered here the initial guesses of $f(\xi)$ is taken as $f(\xi)_{\text{initial}} = 0.0$. We now present below three numerical test cases in determining $f(\xi)$ by the inverse analysis using the CGM.

9.1. Numerical test case 1

The first test case is identical to example 2 in Yang's study [9]. The objective for reconsidering this problem is to proof that the present inverse algorithm is more powerful than the one used in reference [9].

The unknown transient base temperature distribution $f(\xi)$ is assumed as the following form:

$$f(\xi) = 1 + 0.5\cos\left(\frac{\omega\xi}{6.3}\right); \quad 0 \leqslant \xi \leqslant \xi_{\text{f}} \tag{16}$$

The exact function of the base temperature considered in the second example in [7] is not given explicitly, for this reason Eq. (16) is designed as close as possible to the second example considered in [9].

The inverse analysis is first performed by using $\sigma = 0$, $\beta = 2$, $\Delta\xi = 0.1$ and $\Delta\eta = 0.1$. By choosing frequency $\omega =$ 0.1, 0.5 and 1 and using stopping criterion $\varepsilon = 0.0001$, the estimated $f(\xi)$ can be obtained after 14, 17 and 14 iterations, respectively and are shown in Fig. 3.

It should be noted that the estimated base temperatures are not accurate for time near $\xi = 0$. This is due to the fact that the wave is propagated with a finite velocity, and it will not reach the boundary $\eta = 1$ immediately after the base temperature is applied. No temperatures can be measured before the thermal wave reaches $\eta = 1$ and therefore the inverse solutions cannot be solved accurately and uniquely for the initial few time steps.

The computed relative average errors for the estimated base temperature are 0.001671, 0.002248 and 0.001724, respectively and are listed in Table 1, where the relative average error ERR is defined as

$$\text{ERR} = \left[\sum_{m=1}^{M}\left|\frac{f(m) - \hat{f}(m)}{f(m)}\right|\right] \div M \tag{17}$$

Here m represents the index of discreted time, M is the number of the temporal measurements while $\hat{f}(m)$ denotes the estimated values of base temperature.

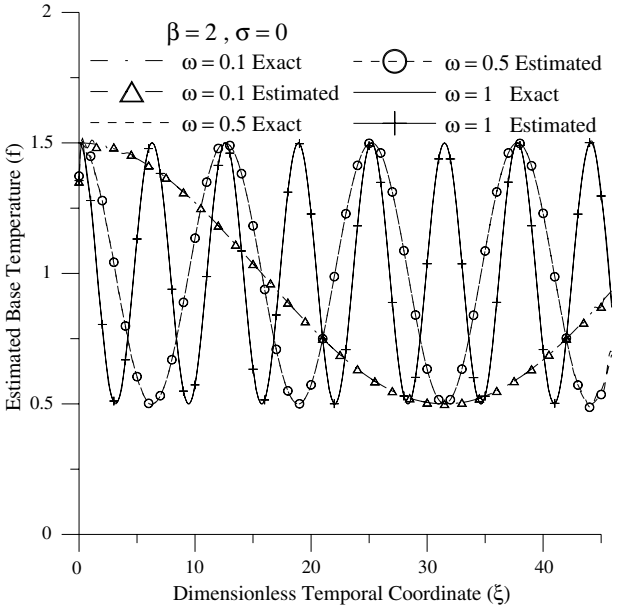

Fig. 3. The exact and estimated results for $\omega = 0.1$, 0.5 and 1 with $\sigma = 0$, $\Delta\eta = 0.1$ and $\Delta\xi = 0.1$ in test case 1.

Table 1
The comparisons of ERR between present study and Yang's results when considering exact measurements

	Relative average error, ERR			
	$\Delta\eta = 0.1$ $\Delta\xi = 0.1$ $\beta = 2$		$\Delta\eta = 0.02$ $\Delta\xi = 0.02$ $\beta = 2$	
	Yang's result [7] with $r = 14$	Present study	Yang's result [7] with $r = 72$	Present study
$\omega = 0.1$	0.002285	0.001671		
$\omega = 0.5$	0.010841	0.002248		
$\omega = 1$	0.022145	0.001724		
$\omega = 2$	0.043757	0.007674	0.003389	0.003325
$\omega = 5$	0.133720	0.006872	0.010825	0.003788

It can be seen from Fig. 3 and Table 1 that the estimated base temperature is very accurate and the use of future time measurements is not needed. The inverse solutions for the above examples are also accurate in [9], but the estimations in this study are more accurate than in [9]. This can be verified from Table 1 since the relative errors for this study are always smaller than Yang's results.

When considering $\omega = 2$ and 5 by Yang [9], the estimated base temperatures deviate from the exact values and the inverse solutions become poor. However, by using the present iterative regularization method with stopping criterion $\varepsilon = 0.0001$, the estimated $f(\xi)$ can be obtained after 12 and 16 iterations for $\omega = 2$ and 5, respectively and the results are shown in Fig. 4. The relative average errors are calculated as 0.007674 and 0.006872, respectively and are also reported in Table 1. It can be learned clearly from the Fig. 4 and Table 1 that the estimations for base temperature with CGM in the present study remain in a good agreement with the exact values.

Yang [9] suggested that a fine mesh is necessary in the periodic temperature input with high frequency, therefore the mesh sizes for time and space are reduced to $\Delta\xi = 0.02$ and $\Delta\eta = 0.02$. Indeed, the estimations are greatly improved when using future time steps in [9], however the optimum number of future time steps is still unknown.

Will the estimations become more accurate when considering reduced mesh sizes with CGM? To answer this question the inverse analysis is performed again with $\Delta\xi = 0.02$ and $\Delta\eta = 0.02$. By using $\varepsilon = 0.0001$, the estimated $f(\xi)$ for $\omega = 2$ and 5 can be obtained after 7 iterations for both cases and the relative average errors can be obtained as 0.003325 and 0.003788, respectively, they are listed in Table 1. It can be seen from the Table 1 that the estimations for this study are also better than those in [9]. The advantage of using CGM is thus proven.

Next, let us discuss the influence of the measurement errors on the inverse solutions. First, the measurement error for the temperatures measured by sensor is taken as $\sigma = 0.05$, then error is increased to $\sigma = 0.1$. The stopping criterion ε is calculated from Eq. (14c) and the number of iterations are 2 and 2 for $\sigma = 0.05$ and $\sigma = 0.1$ with $\beta = 2$. The estimated $f(\xi)$ for $\sigma = 0.05$ and $\sigma = 0.1$ with time are shown in Figs. 5 and 6, respectively and the

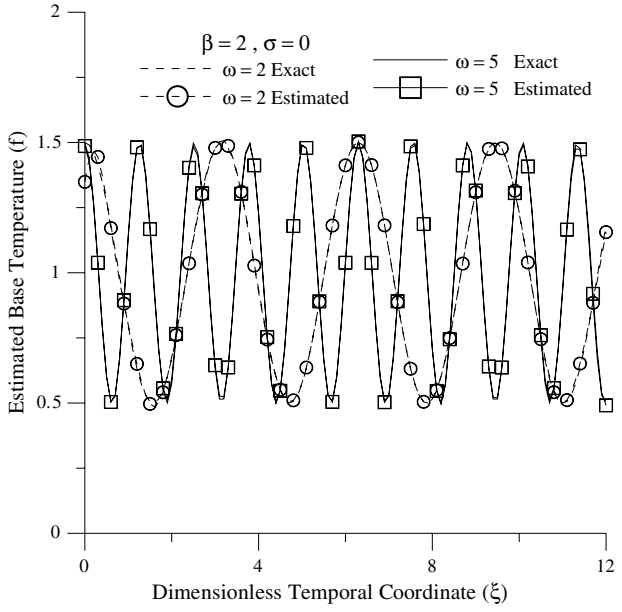

Fig. 4. The exact and estimated results for $\omega = 2$ and 5 with $\sigma = 0$, $\Delta\eta = 0.1$ and $\Delta\xi = 0.1$ in test case 1.

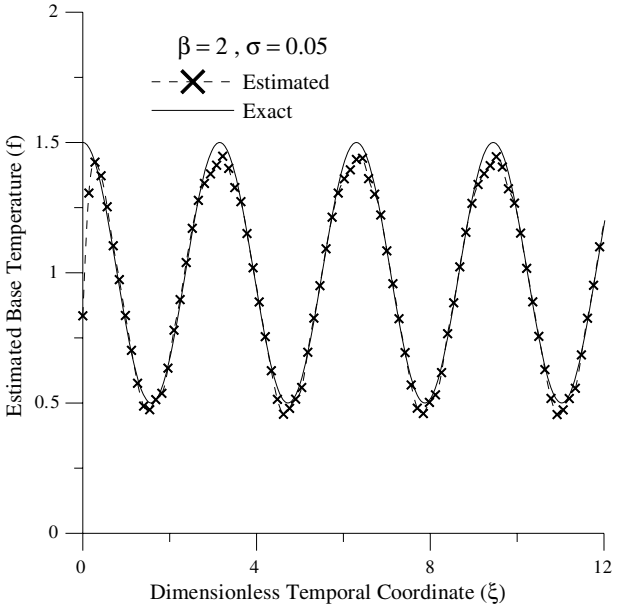

Fig. 5. The exact and estimated results for $\omega = 2$ with $\sigma = 0.05$, $\Delta\eta = 0.02$ and $\Delta\xi = 0.02$ in test case 1.

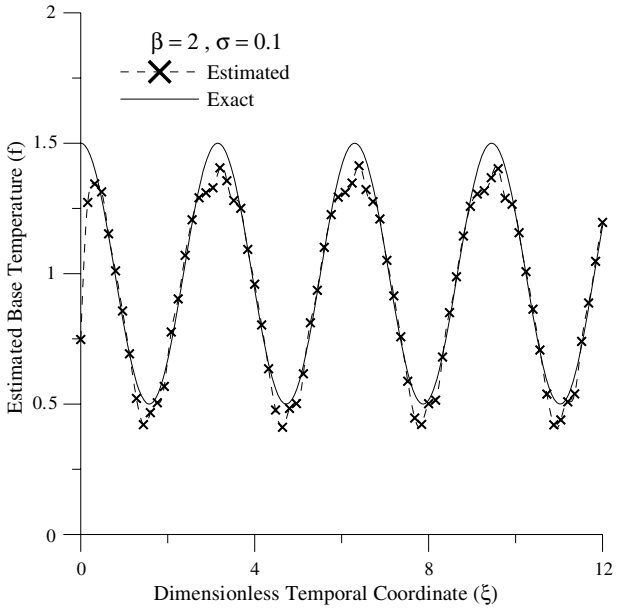

Fig. 6. The exact and estimated results for $\omega = 2$ with $\sigma = 0.1$, $\Delta\eta = 0.02$ and $\Delta\xi = 0.02$ in test case 1.

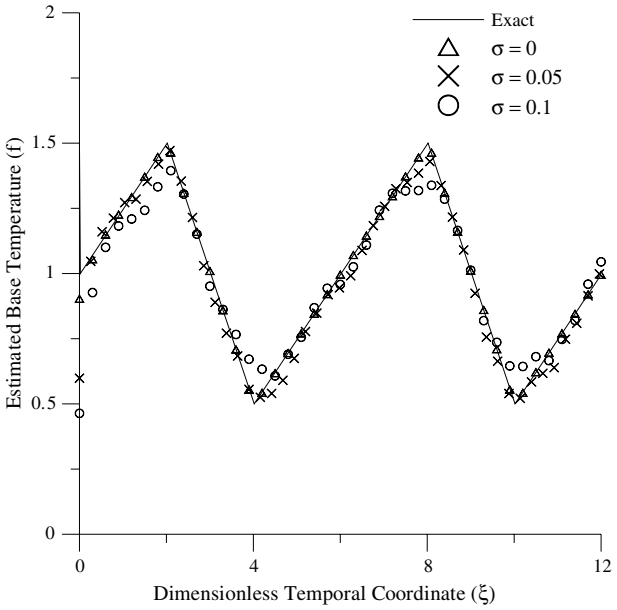

Fig. 7. The exact and estimated results with $\sigma = 0.05$ and 0.1 in test case 2.

Table 2
The comparisons of ERR between present study and Yang's results when considering error measurements

	Relative average error, ERR				
	Using $\Delta\eta = 0.02$ $\Delta\xi = 0.02$ $\omega = 2$ $\beta = 2$				
	Yang's result [7]				Present study
	$r = 72$	$r = 74$	$r = 76$	$r = 78$	
$\sigma = 0.05$	0.087371	0.050208	0.046375		0.032488
$\sigma = 0.1$	0.174555	0.098434	0.080672	0.078355	0.063645

relative average errors are obtained as 0.032488 and 0.063645 and are listed in Table 2.

The inverse estimations involving measurement errors imply that the present algorithm is less sensitive to the measurement error than Yang's [9] since the relative average errors in this article are always smaller than Yang's results. Finally, the reliable inverse solutions can still be obtained when measurement errors are considered.

9.2. Numerical test case 2

The unknown base temperature $f(\xi)$ is assumed as the following triangular shapes:

$$f(\xi) = \begin{cases} 0.5 + 0.5 \times \xi & 0 \leqslant \xi \leqslant 2 \text{ and } 6 < \xi \leqslant 8 \\ 2.5 - 0.5 \times \xi & 2 < \xi \leqslant 4 \text{ and } 8 < \xi \leqslant 10 \\ -0.5 + 0.25 \times \xi & 4 < \xi \leqslant 6 \text{ and } 10 < \xi \leqslant 12 \end{cases} \tag{18}$$

By assuming the conditions $\Delta\xi = 0.02$, $\Delta\eta = 0.02$ and $\sigma = 0.0$, the inverse analysis is performed again. By using stopping criterion $\varepsilon = 0.0001$, after 9 iterations the estimated $f(\xi)$ can be obtained and is shown in Fig. 7. It can be seen from Fig. 7 that the estimation is accurate since the average relative error ERR for estimated base temperature is calculated as ERR = 0.003289.

Next, the measurement error for the temperatures measured by sensor is considering as $\sigma = 0.05$, then it is increased to $\sigma = 0.1$. The number of iterations for $\sigma = 0.05$ and 0.1 are 2 and 1, respectively. The estimated base temperatures $f(\xi)$ for $\sigma = 0.05$ and 0.1 are also shown in Fig. 7 where the relative average error for $\sigma = 0.05$ and 0.1 are 0.037745 and 0.060467, respectively. The results show that by applying this algorithm the inverse solutions are still reliable when measurement errors are considered.

9.3. Numerical test case 3

In the third test case, a more strict shape for the unknown transient base temperature $f(\xi)$ is examined, i.e., the time-dependent base temperature is now assumed as a step function in the following form:

$$f(\xi) = \begin{cases} 1.5 & 0 \leqslant \xi \leqslant 2 \text{ and } 6 < \xi \leqslant 8 \\ 0.5 & 2 < \xi \leqslant 4 \text{ and } 8 < \xi \leqslant 10 \\ 1 & 4 < \xi \leqslant 6 \text{ and } 10 < \xi \leqslant 12 \end{cases} \tag{19}$$

By assuming $\Delta\xi = 0.02$, $\Delta\eta = 0.02$, $\sigma = 0.0$ and choosing $\varepsilon = 0.0001$, the inverse solution for $f(\xi)$ can be obtained after 7 iterations and is shown in Fig. 8. It is clear from Fig. 8 that good estimation is obtained for the base temperatures except for the sharp discontinuity by using the technique of CGM. The average relative error for estimated base temperatures is calculated as ERR = 0.039444.

The influence of the measurement errors on the inverse solutions is then considered. The measurement error for the temperatures is firstly taken as $\sigma = 0.05$, then error is

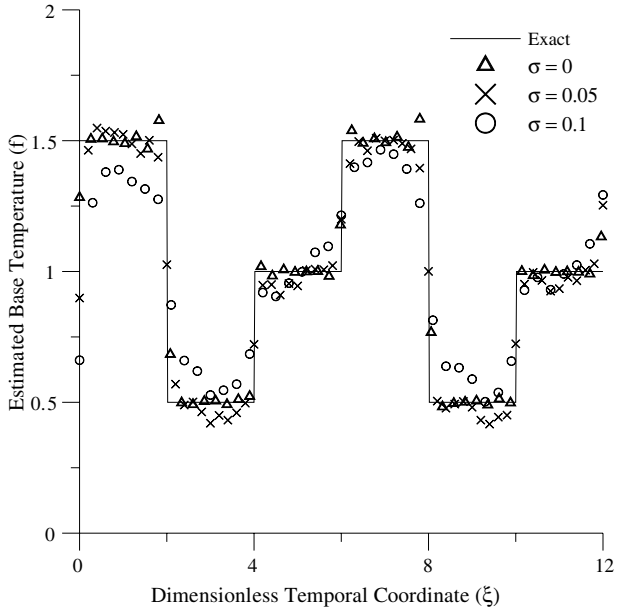

Fig. 8. The exact and estimated results with $\sigma = 0.05$ and 0.1 in test case 3.

increased to $\sigma = 0.1$. The number of iterations for $\sigma = 0.05$ and 0.1 are 2 and 1, respectively. The estimated $f(\xi)$ with time is also shown in Fig. 8, and the relative average errors for $\sigma = 0.05$ and 0.1 are obtained as ERR = 0.075595 and 0.144317, respectively.

From the above three test cases it can be learned that an inverse non-Fourier fin problem in estimating time-dependent base temperature is now completed. Reliable estimations can be obtained when using either exact or error measurements. The drawbacks experienced in reference [9] can be avoided by using the present algorithm.

10. Conclusions

An iterative regularization method, i.e., CGM, was successfully applied for the solution of the inverse non-Fourier fin problems in estimating the unknown transient base temperature based on the simulated temperature readings obtained from the other boundary. Three test cases involving different form of base temperatures and measurement errors were examined. The results show that the inverse solutions obtained by CGM are always better than the algorithm used in Yang's study for the identical problem under consideration. The reliable inverse solutions can still be obtained when large measurement errors were considered.

From the numerical test cases in this study it is concluded that the advantages of using the technique of CGM lie in that (1) the inverse solutions remain stable when the frequency of base temperature is increased, (2) the estimation does not depend on the size of grids, (3) the estimations are not sensitive to the measurement errors and (4) the concept of future time step is not needed in the inverse calculations.

Acknowledgement

This work was supported in part through the National Science Council, ROC, Grant number, NSC-94-2611-E-006-021.

References

[1] A.D. Kraus, Sixty-five years of extended surface technology (1922–1987), Appl. Mech. Rev. 41 (1988) 321–364.
[2] Y.W. Yang, Periodic heat transfer in straight fins, J. Heat Transfer 94 (1972) 310–314.
[3] R.G. Eslinger, B.T.F. Chung, Periodic heat transfer in radiating and convecting fins or fin arrays, AIAA J. 17 (1979) 1134–1140.
[4] B.T.F. Chung, J.R. Iyer, Optimal design of longitudinal rectangular fins and cylindrical spines with variable heat transfer coefficient, Heat Transfer Eng. 14 (1993) 31–42.
[5] R.H. Yeh, Optimum dimensions of longitudinal rectangular fins and cylindrical pin fins with variable heat transfer coefficient, The Canadian J. Chem. Eng. 74 (1996) 144–151.
[6] J.Y. Lin, The non-Fourier effect on the fin performance under periodic thermal conditions, Appl. Math. Model. 22 (1998) 629–640.
[7] V. Isakov, Inverse Problems for Partial Differential Equations, Springer-Verlag, New York, 1998.
[8] V.G. Romanov, Inverse Problems of Mathematical Physics, VNU Science Press, Utrecht, The Netherlands, 1987.
[9] C.Y. Yang, Estimation of the periodic thermal conditions on the non-Fourier fin problem, Int. J. Heat Mass Transfer 48 (2005) 3506–3515.
[10] H. Deng, S. Guessasma, G. Montavon, H. Liao, C. Coddet, D. Benkrid, S. Abouddi, Combination of inverse and neural network methods to estimate heat flux, Numer. Heat Transfer, Part A—Applications 47 (2005) 593–607.
[11] J. Su, G.F. Hewitt, Inverse heat conduction problem of estimating time-varying heat transfer coefficient, Numer. Heat Transfer, Part A—Applications 45 (2004) 777–789.
[12] S.M.H. Sarvari, S.H. Mansouri, J.R. Howell, Inverse boundary design radiation problem in absorbing-emitting media with irregular geometry, Numer. Heat Transfer, Part A—Applications 43 (2003) 565–584.
[13] C.H. Huang, J.H. Hsiao, An inverse design problem in determining the optimum shape of spine and longitudinal fin, Numer. Heat Transfer, Part A—Applications 43 (2003) 155–177.
[14] R. Sampath, N. Zabaras, Adjoint variable method for the thermal design of eutectic directional solidification processes in an open-boat configuration, Numer. Heat Transfer, Part A—Applications 39 (2001) 655–683.
[15] M.J. Colaço, H.R.B. Orlande, Inverse forced convection problem of simultaneous estimation of two boundary heat fluxes in irregularly shaped channels, Numer. Heat Transfer, Part A—Applications 39 (2001) 737–760.
[16] C.H. Huang, S.C. Cheng, A three-dimensional inverse problem of estimating the volumetric heat generation for a composite material, Numer. Heat Transfer, Part A—Applications 39 (2001) 383–403.
[17] M. J Colaço, H.R.B. Orlande, Comparison of different versions of the conjugate gradient method of function estimation, Numer. Heat Transfer, Part A—Applications 36 (1999) 229–249.
[18] C.H. Huang, H.M. Chen, Inverse geometry problem of identifying growth of boundary shapes in a multiple region domain, Numer. Heat Transfer, Part A—Applications 35 (1999) 435–450.
[19] M. Prud'homme, T.H. Nqugyen, Whole time-domain approach to the inverse natural convection problem, Numer. Heat Transfer, Part A—Applications 32 (1997) 169–186.
[20] A.J.S. Neto, M.N. Ozisik, simultaneous estimation of location and timewise-varying strength of a plane heat source, Numer. Heat Transfer, Part A—Applications 24 (1993) 467–477.

[21] C.H. Huang, M.N. Ozisik, Inverse problem of determining unknown wall heat flux in laminar flow through a parallel plate duct, Numer. Heat Transfer, Part A—Applications 21 (1992) 55–70.
[22] O.M. Alifanov, Inverse Heat Transfer Problems, Springer-Verlag, Berlin Heidelberg, 1994.
[23] C.H. Huang, S.P. Wang, A three-dimensional inverse heat conduction problem in estimating surface heat flux by conjugate gradient method, Int. J. Heat Mass Transfer 42 (1999) 3387–3403.
[24] C.H. Huang, W.C. Chen, A three-dimensional inverse forced convection problem in estimating surface heat flux by conjugate gradient method, Int. J. Heat Mass Transfer 43 (2000) 3171–3181.
[25] C.H. Huang, C.Y. Huang, An inverse biotechnology problem in estimating the optical diffusion and absorption coefficients of tissue, Int. J. Heat Mass Transfer 47 (2004) 447–457.
[26] C.H. Huang, H.C. Lo, A three-dimensional inverse problem in predicting the heat fluxes distribution in the cutting tools, Numer. Heat Transfer, Part A—Applications 48 (2005) 1009–1034.
[27] C.H. Huang, C.C. Shih, A shape identification problem in estimating simultaneously two interfacial configurations in a multiple region domain, Appl. Therm. Eng. 26 (2006) 77–88.
[28] G.F. Carey, M. Tsai, Hyperbolic heat transfer with reflection, Numer. Heat Transfer 5 (1982) 309–327.
[29] L.S. Lasdon, S.K. Mitter, A.D. Warren, The conjugate gradient method for optimal control problem, IEEE Trans. Autom. Control AC-12 (1967) 132–138.
[30] IMSL Library Edition 10.0. User's Manual: Math Library Version 1.0, IMSL, Houston, TX, 1987.